Hydrogen-Bonding in Ethanol Adducts to Bis(3-*R*-penta-2,4-dionato)Nickel(II) Species

Valery R. Polyakov*

Max-Planck-Institut für Kohlenforschung, Kaiser-Wilhelm-Platz 1, D-45470 Mülheim an der Ruhr, Germany

Marian Czerwinski

Institute of Chemistry, Pedagogical University Czestochowa, 42−200, Poland

Received November 2, 1999

Ethanol adducts of bis(3-*R*-penta-2,4-dionato) nickel(II) have been prepared by recrystallization of the corresponding nickel bisacetylacetonate species from ethanol, and their crystal structures have been determined by X-ray diffraction: R = methyl, $C_{16}H_{30}NiO_6$, $a = 5.177(1)$, $b = 9.326(1)$, $c = 9.649(1)$, $a = 95.39(1)$, $\beta = 100.04(1)$, $\gamma = 97.16(1)$, space group $P\bar{1}$, $Z = 1$; R = hex-5-enyl, $C_{26}H_{46}NiO_6$, $a = 5.176(1)$, $b = 9.677(1)$, $c = 14.458(1)$, $a = 92.333(3)$, $\beta = 93.945(4)$, $\gamma = 96.011(6)$, space group $P\bar{1}$, $Z = 1$; R = phenyl, $C_{26}H_{34}NiO_6$, $a = 27.399(1)$, $b = 5.349(1)$, $c = 19.827(2)$, $\beta = 117.410(7)$, space group $C2/c$, $Z = 4$. The compounds show remarkable differences in their ability to form hydrogen bonds in the solid phase and in solution, depending upon the nature of the substituent in the 3-position of the acetylacetone fragment. Analysis of the strength of hydrogen bonds within the limits of supermolecular approximation based on the results of calculations by DFT method has been carried out and were found to correlate with experimental observations.

Introduction

In a previous publication,[1] we suggested that substituents in the 3-position of 2,4-diketonates have a significant influence on the tendency of 3-substituted bis-2,4-diketonates of nickel to adopt either a monomeric or a trimeric structure as the result of electronic effects associated with the substituent. Both mono- and trimeric 3-substituted penta-2,4-dionato derivatives of nickel(II) readily form adducts with ethanol, and herein we report the effect of the substituent upon the structure and reactions of these species and compare them to the known example $Ni(acac)_2 \cdot 2EtOH$(**4**).[2]

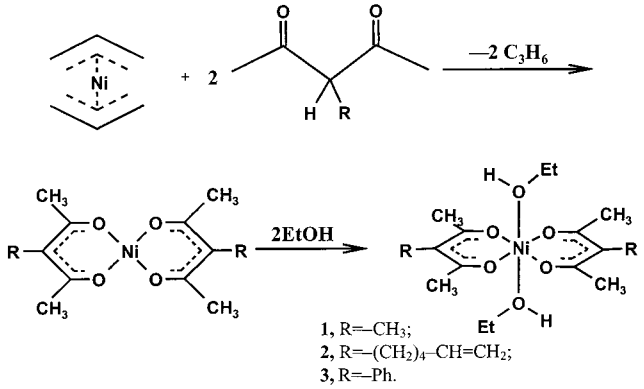

Experimental Section

General Techniques. Infrared spectra (KBr pellets) have been recorded on a Nicollet Magna−IR 750 spectrophotometer in the range of 4000−400 cm^{-1}. Mass spectra have been recorded on a Finigan MAT 8200 using an EI method with 70 eV ionization energy. UV−Vis spectra have been recorded on a Varian CARY 2300 UV−Vis−NIR spectrophotometer in the Helma Q5 cells. The general experimental conditions have been described earlier.[3]

The bis(3-*R*-penta-2,4-dionato)nickel(II) complexes and **3** were prepared previously.[1] **1** and **2** were prepared as green crystals in quantitative yield by recrystallizing the corresponding bis(3-*R*-penta-2,4-dionato)nickel(II) complexes from absolute ethanol. Satisfactory analytical (elemental analyses, MS) data could not be obtained since the compounds readily eliminate ethanol, reforming the pink starting material. However, the IR spectra (Table 1) clearly show the formation of an ethanol adduct.

X-ray Crystallography. Details of the crystal data and refinement for the compounds studied are given in Table 2. The atomic coordinates have been deposited with the other Supporting Information. Crystals were sealed in glass capillaries under argon. Intensity data collection was carried out using an Enraf-Nonius CAD-4 automatic diffractometer using graphite-monochromatic Cu Kα radiation by a coupled $\omega - 2\theta$ scan technique. Unit cell parameters were determined by the least-squares from 25 reflections, and data reduction was performed by DATAP.[4] Because of the low absorption coefficients, absorption corrections have not been applied. All structures were solved by direct methods using SHELXS-86[5] and refined by full-matrix, least-squares on all F_o^2 using SHELXL-93.[6] All non-hydrogen atoms were refined anisotropically. All hydrogen atoms have been found from the difference Fourier maps and isotropically included in the subsequent least-squares refinements. The correct choice of the more symmetrical space groups for **1**, **2**, and **3** was confirmed by the subsequent refinements.

Theoretical Methods. The calculations with full optimization were based on the DFT method implemented in the GAUSSIAN-94

* To whom correspondence should be addressed. Current address: ChemCodes Inc., 2300 Englert Drive, Suite G, Durham, NC 27713. E-mail: valery.polyakov@writeme.com

(1) Döhring, A.; Goddard, R.; Jolly, P. W.; Krüger, C.; Polyakov, V. R. *Inorg. Chem.* **1997**, *36*, 177−183.
(2) Pfluger, C. E.; Burke, T. S.; Bednowitz, A. L. *J. Cryst. Mol. Struct.* **1973**, *3*, 181−91.
(3) Goddard, R.; Hopp, G.; Jolly, P. W.; Krüger, C.; Mynott, R.; Wirtz, C. *J. Organomet. Chem.* **1995**, *163*, 486.
(4) Coppens, P.; Leiserowitz, L.; Rabinovich, D. *Acta Crystallogr., Sect. A*: **1965**, *18*, 1035.
(5) Sheldrick, G. M. *Acta Crystallogr., Sect. A*: **1990**, *46*, 467.
(6) Sheldrick, G. M. SHELXL-93 University of Göttingen, 1993.

10.1021/ic991284v CCC: $20.00
Published on Web 07/27/2001

Table 1. Infrared Data for **1**−**4** (KBr, RT, cm^{-1})

compound	$\nu_{C=CH}$	$\nu_{C-H(aliph.)}$	$\nu_{C=C}$	$\nu_{O=C-C-C=O}$	$\nu_{C=CH/Ph}$	ν_{OH}
1	−	2970, 2960, 2930	−	1590, 1380	−	3250
2	3080	2922, 2854	1641	1597,1447, 1384	1004, 909	3423
3	3084, 3060, 3025	2954, 2925	1515	1585, 1421, 1385	1011, 921, 767, 704	3387
4	3077	2990, 2925	1655	1617, 1520, 1464, 1402	1021, 934	3426

Table 2. Crystallographic Data for **1**−**3**[a]

compound	**1**	**2**	**3**
empirical formula	$C_{16}H_{30}NiO_6$	$C_{26}H_{46}NiO_6$	$C_{26}H_{34}NiO_6$
FW	377.11	513.34	501.24
temp, K	98(2)	293(2)	293(2)
wavelength, Å	1.54178	1.54178	1.54178
Space group (number)	$P\bar{1}$ (2)	$P\bar{1}$ (2)	$C2/c$ (15)
a, b, c (Å)	5.177(1), 9.326(1), 9.649(1)	5.176(1), 9.677(1), 14.458(1)	27.399(1), 5.349(1), 19.827(2)
α, β, γ (°)	95.39(1), 100.04(1), 97.16(1)	92.333(3), 93.945(4), 96.011(6)	90, 117.410(7), 90
vol, ($Å^3$)	451.95(11)	717.6(2)	2579.6(6)
Z	1	1	4
calcd density (Mg/mm^3)	1.386	1.188	1.291
abs coeff (mm^{-1})	1.779	1.247	1.387
Final R1, wR2 [$I > 2\sigma(I)$]	0.0375, 0.1028	0.0446, 0.1216	0.0494, 0.1418
R1, wR2 (all data)	0.0378, 0.1032	0.0467, 0.1239	0.0593, 0.1482

[a] $R(int) = \sum|F_o^2 - F_o^2\,(mean)|/\sum|F_o^2|$; $R1 = \sum(|F_o| - |F_c|)/\sum|F_o|$; $wR2 = \{\sum[w(F_o^2 - F_c^2)^2]/\sum[w(F_o^2)^2]\}^{0.5}$; $S = \{\sum[w(F_o^2 - F_c^2)^2]/(n - p)\}^{0.5}$; where: F_o = observed structure factors, F_c = calculated structure factors, w = weighting scheme (see instructions to SHELXL-93), n = number of elections, p = total number of parameters refined. Corrections for extinction used the expression: $F_c^{new} = kF_c[1 + 0.001\,eF_c^2\lambda^3/\sin(2\theta)]^{-0.25}$.

program.[7] The Lanl2dz double-ζ basis set,[8] Becke three-parameter functional (B3LYP),[9] and Berny geometry-optimization algorithm[10] were used.

DMol quantum chemistry software package[11] was used to calculate density distribution expressed in a numerical atomic orbital. Local correlation functional of Vosko−Wilk−Nusair[12] VWN type included "nonlocal" usage of the gradient corrected exchange Becke's 1988 version B88[13] and corrected correlation energies LYP.[14] Calculations were performed with nonfrozen orbitals.

All the numerical calculations were carried out using Cray J90 and Cray Y-MP supercomputers.

Discussion

Several effects are apparent when comparing the crystal structures of **1** (R═CH_3), **2** (R═$(CH_2)_4$−CH═CH_2), **3** (R═Ph), and that of the only known compound of this type **4**[2] (R═H). (1.) The molecules interact with each other through intermolecular hydrogen bonds. (2.) The acetylacetone fragment is nonplanar, and the degree of bending depends on the nature of the substituent **R**.

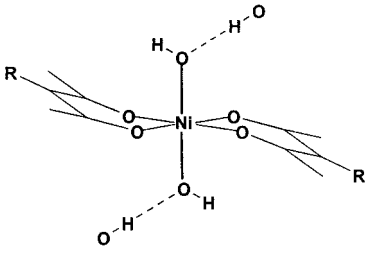

(3.) The complexes have an anomalous order of stability; those with the stronger Ni−O (EtOH) bond eliminate ethanol at much lower temperatures than those with weaker bonds.

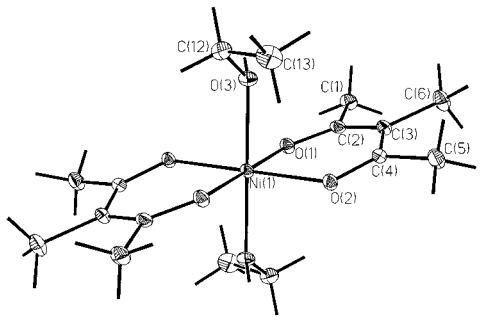

Figure 1. Molecular structure of bis(ethanol)-bis(3-methylpenta-2,4-dionato)nickel(II) (**1**) (40% probability level).

The H-bonds have been analyzed using oxygen−oxygen separation criteria rather than considering pairs of O···H and H−O distances because of the low accuracy in determining the positions of hydrogen atoms, which makes a direct comparison based on hydrogen−oxygen separation impossible. According to the Hamilton and Ibers criteria,[15] H-bonding between two atoms exists if the separation between them is less than the sum of their Pauling van der Waals radii (1.4 Å for oxygen). However, this approach has been criticized by Jeffrey and Saenger[16] as being too restrictive, and these authors have introduced a criterion based on the sum of Allinger van der Waals radii (1.65 Å for the oxygen).

The molecular structures of **1**−**3** are shown in the Figures 1−3; selected bond distances and bond angles are listed in the Tables 3 and 4. The crystal structures of **1**−**3** have much in common with that of **4**[2]; the nickel atom has an octahedral environment, with the four oxygen atoms of the pentadionato fragment lying in the equatorial plane and two ethanol oxygen atoms in the axial positions. The Ni−O bond distances are 2.0−2.1 Å.

(7) *GAUSSIAN 94, Revision D.3*; Gaussian, Inc.: Pittsburgh, PA, 1995.
(8) (a) Hay, P. J.; Wadt, W. R. *J. Chem. Phys*. **1985**, *82*, 270−299. (b) Wadt, W. R.; Hay, P. J. *J. Chem. Phys*. **1985**, *82*, 284.
(9) (a) Becke, A. D. *J. Chem. Phys*. **1988**, *88*, 52. (b) Lee, C.; Yang, W.; Parr R. G. *Phys. Rev. B*: **1988**, *37*, 786. (c) Becke A. D. *J. Chem. Phys*. **1993**, *98*, 5648.
(10) Schlegel, H. B. *J. Comput. Chem*. **1982**, *3*, 214.
(11) *DMol Version 2.3.0*; Biosym Technologies Inc., 1993.
(12) Vosko, S. J.; Wilk, L.; Nusair, M. *J. Phys*. **1980**, *58*, 1200.
(13) Becke, A. D. *J. Chem. Phys*. **1988**, *88*, 52.
(14) Lee, C.; Yang, W.; Parr, R. G. *Phys. Rev. B*: **1988**, *37*, 786.
(15) Hamilton, W. C.; Ibers, J. A. *Hydrogen bonding in solids*; W. A. Benjamin: New York, 1968.
(16) Jeffrey, G. A.; Saender, W. *Hydrogen Bonding in Biological Structures*, Springer-Verlag: Berlin, Heidelberg, 1991.

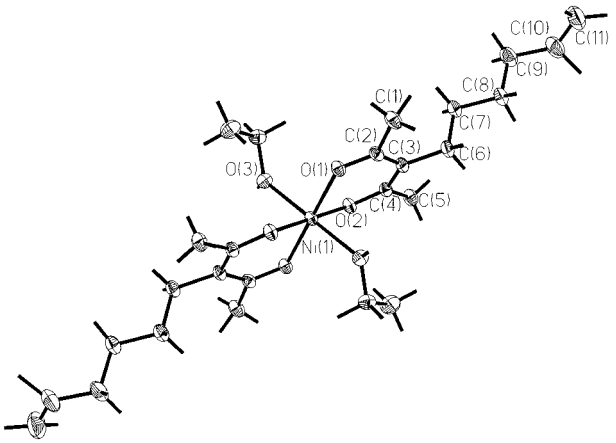

Figure 2. Molecular structure of bis(ethanol)-bis(3-1-hexenylpenta-2,4-dionato)nickel(II) (**2**) (20% probability level).

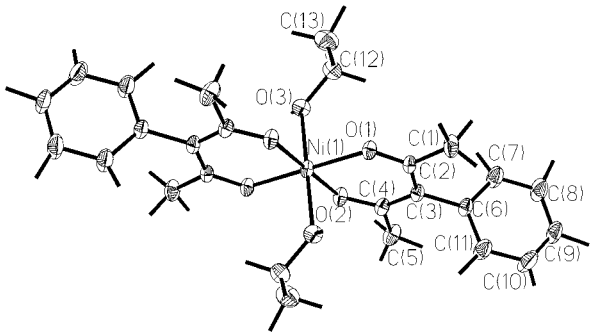

Figure 3. Molecular structure of bis(ethanol)-bis(3-phenylpenta-2,4-dionato)nickel(II) (**3**) (20% probability level).

Table 3. Selected Bond Distances (Estimated) for **1**−**3** (Å)

fragment	bond	**1**	**2**	**3**
coord. environment at Ni^{2+}	Ni(1)−O(1)	1.997(1)	1.989(1)	1.977(2)
	Ni(1)−O(2)	2.002(1)	2.000(1)	1.998(2)
	Ni(1)−O(3)	2.106(1)	2.115(1)	2.139(2)
	Ni(1)−O(4)	−	−	−
	Ni(1)−O(4a)	−	−	−
	Ni(1)−O(4b)	−	−	−
acetylacetone fragment	O(1)−C(2)	1.264(2)	1.265(2)	1.261(3)
	O(2)−C(4)	1.279(2)	1.278(2)	1.273(3)
	C(1)−C(2)	1.518(2)	1.513(3)	1.513(4)
	C(2)−C(3)	1.419(2)	1.412(3)	1.409(4)
	C(3)−C(4)	1.408(2)	1.410(2)	1.406(4)
	C(4)−C(5)	1.512(2)	1.500(3)	1.509(4)
	C(3)−C(6)	1.518(2)	1.518(2)	1.509(3)
	C(3)−Cl(1)	−	−	−
ethanol fragment	O(3)−C(12)	1.432(2)	1.431(2)	1.427(4)
	C(12)−C(13)	1.503(3)	1.480(4)	1.456(5)
ethylato- fragment	O(4)−C(14)	−	−	−
	C(14)−C(15)	−	−	−
substituent	C(6)−C(7)	−	1.522(3)	1.384(4)
	C(7)−C(8)	−	1.524(3)	1.398(4)
	C(8)−C(9)	−	1.514(4)	1.365(6)
	C(9)−C(10)	−	1.516(4)	1.319(6)
	C(10)−C(11)	−	1.223(6)	1.389(5)
	C(6)−C(11)	−	−	1.356(4)
H-bonding	O(3)···O(2b)	2.710(2)[a]	2.726(2)[b]	2.825(3)[c]

[a] $x - 1, y, z$. [b] $-x + 1, -y, -z$. [c] $-x + 1/2, -y + 3/2, -z$.

The compounds **1**−**4** can be divided into two classes depending upon the nature of the substituent on the acetylacetone ligand, which is likely to determine the strength of the H-bonds between two neighboring molecules (Figure 4) in the crystal. Compounds **1** and **2**, with electron-donating substituents, have strong H-bonding associated with oxygen−oxygen separations

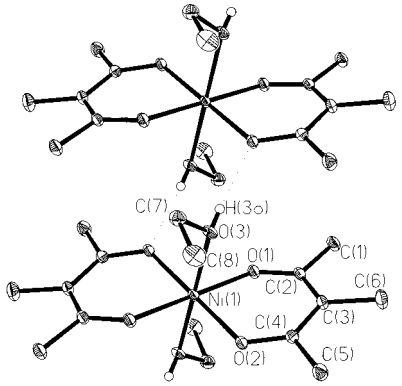

Figure 4. Intermolecular hydrogen bonding (dotted lines) in ethanol complexes (**1**) (40% probability level). Hydrogen atoms other then attached to oxygens were omitted for clarity.

of 2.710(2) and 2.726(2) Å, respectively. The compounds **3** and **4**, without such substituents, have oxygen−oxygen separations in excess of 2.82 Å (Table 3 and [2]) and exhibit much weaker H-bonding.

While the geometry of all four complexes is similar, with almost identical coordination environments at the nickel atom, there are significant differences in details. Comparing compounds **2** and **3**, measured at the same temperature and having electron-donating and electron-accepting substituents, respectively, one can observe slightly shorter Ni−O equatorial distances for compound **3**. This, according to reference 17 (using this reference was suggested by the referee), results in an increase of the axial Ni−O bond length from 2.115(1) Å (for **2**) to 2.139(2) Å (for **3**). Electron-donating substituents make O(2) atoms better proton acceptors, while the shorter Ni−O3 bonds in these cases should result in looser O(3)−H interactions. As a result, one can observe shorter O···O distances for **1** and **2** and, therefore, stronger H-bonding interactions.

Effects related to the H-bonding have also been noticed in solution. A comparison of the UV−vis spectra of **1**−**4** in ethanol and pentane solutions reveals that the H-interaction charge-transfer band, which for **1** and **2** can be observed in ethanol at ca. 290−330 nm, is no longer visible for their solutions in pentane. In the case of **3** and **4**, the charge-transfer band is observed neither in pentane nor in ethanol.

Substituents' effect and H-bonding also leads to other changes in the geometry of the molecules. In the case of $Ni(acac)_2 \cdot 2EtOH$ (**4**), the nickel atom and the four equatorial oxygen atoms are located in the plane of the acetylacetone fragments, while for **1** and **2** they adopt interplanar angles (between Ni and oxygen plane and the plane of the acetylacetone fragment shown above) of 17° and 20°, respectively. A possible explanation is that of H-bonding with participation of a lone electron pair of the O(2) atom and rehybridization toward sp^3. Compound **3** also exhibits weak H-bonds in the solid state. The nonplanarity of this compound could be the result of an interaction of the phenyl group with the acetylacetone fragment as discussed earlier.[1] The phenyl group is twisted by ca. 78° out of the molecular plane, while C3−C6 is significantly shorter than in the other examples (Table 3).

The tendency to eliminate ethanol molecules is also unusual for these complexes. One would expect that the compounds with the shorter axial Ni−O bonds (**1** and **2**) would lose ethanol at higher temperatures than those having a longer axial Ni−O bond (**3** and **4**). However, during the TGA analysis, it was found that

(17) See, R. F.; Kruse, R. A.; Strub, W. M.; *Inorg. Chem.* **1998**, *37*, 5369−5375.

Table 4. Selected Bond Angles (Estimated) for **1**−**3**([0])

fragment	angle	1	2	3
coordination environment at Ni^{2+}	O(1)−Ni(1)−O(2)	88.71(5)	87.29(5)	88.75(7)
	O(1)−Ni(1)−O(2a)	91.29(5)[a]	92.71(5)[a]	91.25(7)[b]
	O(1)−Ni(1)−O(3)	86.26(5)	91.99(6)	93.22(8)
	O(2)−Ni(1)−O(3)	89.88(5)	90.06(6)	89.18(8)
	O(1)−Ni(1)−O(3a)	93.74(5)[a]	88.01(6)[a]	86.78(8)[b]
	O(2)−Ni(1)−O(3a)	90.12(5)[a]	89.94(6)[a]	90.82(8)[b]
acetylacetone fragment	C(2)−O(1)−Ni(1)	125.8(1)	126.3(1)	128.0(2)
	C(4)−O(2)−Ni(1)	125.9(1)	125.0(1)	126.8(2)
	O(1)−C(2)−C(3)	126.5(2)	125.9(2)	126.0(2)
	O(1)−C(2)−C(1)	114.6(2)	113.7(2)	113.1(2)
	C(3)−C(2)−C(1)	119.0(2)	120.3(2)	120.9(2)
	C(4)−C(3)−C(2)	122.3(2)	121.5(2)	122.5(2)
	C(4)−C(3)−C(6)	119.3(2)	119.2(2)	118.7(2)
	C(2)−C(3)−C(6)	118.3(2)	119.3(2)	118.8(2)
	O(2)−C(4)−C(3)	125.5(2)	125.4(2)	125.6(2)
	O(2)−C(4)−C(5)	114.3(2)	113.4(2)	113.4(2)
	C(3)−C(4)−C(5)	120.2(2)	121.2(2)	121.0(2)
ethanol fragment	C(12)−O(3)−Ni(1)	124.1(1)	126.0(1)	124.9(2)
	O(3)−C(12)−C(13)	109.5(2)	110.6(2)	110.8(3)
substituent	C(6)−C(7)−C(8)	−	111.8(2)	120.9(4)
	C(9)−C(8)−C(7)	−	114.2(2)	120.0(4)
	C(10)−C(9)−C(8)	−	111.3(3)	119.2(3)
	C(9)−C(10)−C(11)	−	128.0(4)	121.5(4)
	C(6)−C(11)−C(10)	−	−	121.6(4)
	C(11)−C(6)−C(3)	−	−	122.4(3)
	C(11)−C(6)−C(7)	−	−	116.7(3)

[a] $-x, -y, -z$. [b] $-x + 1/2, -y + 1/2, -z$.

1 and **2** begin to eliminate ethanol at room temperature, while **3** and **4** must be warmed to 80 °C. A possible explanation for this fact is that the products of the thermolysis are different; **1** and **2** eliminate ethanol to give a pink monomer whereas **3** and **4** give a green trimer.[1,2]

The bond-valence model of hydrogen bonding, published by Brown[18] and others, is well established in inorganic chemistry. Some later papers provide a detailed analysis of hydrogen bonds based on either on X-ray[17,19,20] or low-temperature neutron diffraction data.[21] For a detailed discussion about computing hydrogen bonds, see references 22 and 23.

Full optimization passed for the complexes **1** and **3**. Initial positions of ethanol fragments were chosen so that all of the nickel−oxygen distances in the molecules were the same (260 nm). The system Hessian with $(3n - 6)$ eigenvalues confirms that the minimum energies were found for **1**. Finally, the process of optimization of compound **1** led to a structure with hydrogen bonds (Figure 5). Calculation of H-bond energy is also confirmed by the density distribution contained in Table 5. The calculated length for the hydrogen bond is 275 nm (Figure 6), and the average energy calculated after the optimization (according to eq 1) is 9.73 kcal/mol.

$$\Delta E_{\mathrm{H-bond}} = 0.5(E_{\mathrm{str}} - E_{\mathrm{str-2eth}} - 2E_{\mathrm{eth}}) \qquad (1)$$

$\Delta E_{\mathrm{H-bond}}$ is the average energy of hydrogen bonds (Table 6), E_{str} is the total energy of the structure after optimization, $E_{\mathrm{str-2eth}}$ is the total energy of the structure without ethanol fragments after optimization, and E_{eth} is the total energy of ethanol fragments after optimization = −155,02248 au.

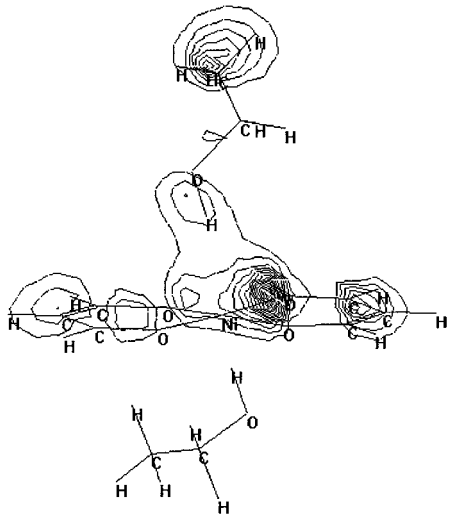

Figure 5. Molecular orbital (−0.2758 au) on the hydrogen atom of ethanol fragment (structure **1**).

Table 5. Effective Atomic Charge for Mulliken Population for **1** and **3** after and before (in Parentheses) Complex Formation with Full Optimization Based on the DFT B3LYP Method with the Lanl2dz Double-ζ Basis Set

no.	atoms	1	3
1	O (from OH−Et)	−0.536 (−0.483)	−0.462 (−0.483)
2	H(from HO−Et)	0.411 (0.335)	0.346 (0.335)
3	Ni	0.459 (0.505)	0.340 (0.502)
4	O1(from acc[a])	−0.417 (−0.347)	−0.330 (−0.348)
5	O2(from acc[a])	−0.358 (−0.347)	−0.341 (−0.348)
6	H (from Et−OH)	0.232 (0.221)	0.190 (0.220)
7	C(from Et−OH)	−0.631 (−0.618)	−0.548 (−0.618)

[a] Acetylacetone fragment.

For compound **3**, it was also possible to perform full optimization using similar starting conditions (all nickel−oxygen distances have the same length of 260 nm). During the optimization process, ethanol fragments drifted away from acetylacetone fragments (Figure 6). Calculated bonding energy of ethanol to acetylacetone fragment (even when O···H−O−

(18) Brown, I. D. *Acta Crystallogr.* **1992**, *B48*, 553−572.
(19) Gilli, P.; Bertolasi, V.; Ferretti, V.; Gastone, G. *J. Am. Chem. Soc.* **1994**, *116*, 909−915.
(20) see: R. F.; Curtis, C. J.; McConnell, K. W.; Santhraman, S.; Strub, W. M.; Ziller, J. W. *Inorg. Chem.* **1997**, *36*, 4151−4155.
(21) Steiner, Th.; Saenger, W. *Acta Crystallogr.* **1994**, *B50*, 348−357.
(22) Kar, T.; Scheiner, S.; Cuma, M. *J. Chem. Phys.* **1999**, *111*, 849−858.
(23) Kumar, G. A.; Yongping Pan; Smallwood, C. J.; McAllister, M. A. *J. Comput. Chem.* **1998**, *19*, 1345−1352.

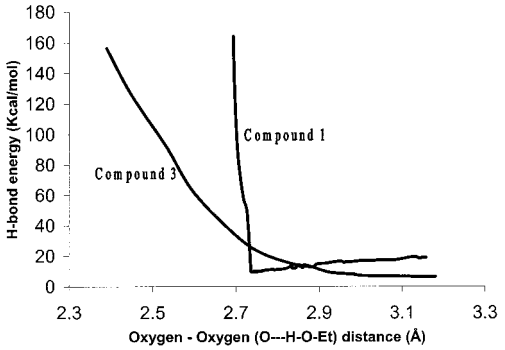

Figure 6. Hydrogen bond energy as a function of oxygen−oxygen distance for the compounds **1** and **3**.

Table 6. H-Bond Energies[a] (a.u.) for **1** and **3** (Eq 1)

compound	H-bond energies	E_{str}	$E_{str-2eth}$
1	−0.03104	−1012.51791	−702.44191
3	0.01017	−1474.51192[b]	−1164.48730

[a] Hydrogen bond energies were calculated using a procedure called "supermolecular approach": (1) Van Duijneveldt-van de Rijdt, J. G. C. M.; van Duijneveldt, F. B. In *Theoretical Treatment of Hydrogen Bonding*; Chapter 2. (2) D. Hadz i, Ed., John Wiley, New York, 1997. (3) Narbutt, J.; Czerwiñski, M.; Krejzler, J. *Eur. J. Inorg. Chem.* **2001**, in press. [b] E_{str} = the total energy when O−H−O Et distance = 312 nm.

Et distance is 312 nm) is positive (Table 6). This allowed us to ascertain that hydrogen bonds cannot be created. Computed stability of hydrogen bonds for **1** and **3**, therefore, correlates with the experimental X-ray data and theoretical explanations given above.

The studies[24] of the electron density distribution for systems with hydrogen bonds lead to the following conclusions (Table 5). First, formation of a hydrogen bond decreases the electron density on the H atom participating in the bond and increases the electron density on donor and acceptor atoms, with the greater increase on the donor atom. Second, the electron density of all other hydrogen atoms connected to the proton donor increase. Third, these changes in the electron density on atoms connected to atoms forming a hydrogen bond are of the same order as those for atoms directly participating in the bond. Plots of the distribution of the electron density show a decrease of density in the proximity of the O···H system (Figure 5).

One can observe similar changes in charge distribution by analyzing results of calculations performed by freezing the geometry of the optimized acetylacetone fragment for the compounds **1** and **2** during the formation of the complex (Table in the Supporting Information). We have also computed the charge distribution for **3** and **4** with and without EtOH using DFT method from the DMol quantum chemistry software package (see Table in the Supporting Information).

(24) Shuster, P.; Lischka, H.; Beyer, A., In *Applications of MO Theory in Organic Chemistry*; Czizmadia, I. G., Ed.; Elsevier: Amsterdam, 1977; p 89.

Conclusions

Our results suggest that the remote substituent in the 3-position of the 2,4-diketonate can strongly affect the geometry around the nickel atom and the chemical properties of the alcohol adducts of the described nickel complexes, as well as their ability to form hydrogen bonds in the solid phase and solution. Calculations carried out by using DFT method are in an excellent agreement with the experimental data and fully support the above statements. These calculations also indicate that the Hamilton−Ibers criterion can more appropriately characterize the hydrogen bonding in the described systems than that proposed by Jeffrey and Saenger.

Acknowledgment. We gratefully acknowledge assistance of Prof. P. W. Jolly in the preparation of this manuscript. Numerical calculations were carried out in part at the Interdisciplinary Centre for Mathematical and Computational Modeling (Warsaw, Poland) and Poznan Supercomputing Centre.

Supporting Information Available: Results from ab initio and DFT methods for calculation of the atomic charges, and an X-ray crystallographic file in CIF format for the structure determinations of compounds **1**, **2**, and **3**. This material is available free of charge via the Internet at http://pubs.acs.org.

IC991284V